Snapshot Mueller matrix spectropolarimeter

Nathan Hagen,[1,*] Kazuhiko Oka,[2] and Eustace L. Dereniak[1]

[1]*College of Optical Sciences, University of Arizona, 1630 East University Boulevard, Tucson, Arizona 85721, USA*
[2]*Graduate School of Engineering, Division of Applied Physics, Hokkaido University, Sapporo 060-8628, Japan*
**Corresponding author: nhagen@optics.arizona.edu*

Received April 9, 2007; revised May 17, 2007; accepted May 24, 2007;
posted May 29, 2007 (Doc. ID 81899); published July 19, 2007

We present a new snapshot technique for performing spectrally resolved Mueller matrix polarimetry. The basic approach is an extension of the channeled spectropolarimetry technique, employing frequency-domain interferometry to encode polarization information into modulation of the spectrum. © 2007 Optical Society of America

OCIS codes: 120.2130, 120.5410, 260.5430, 300.6190.

Mueller matrix polarimeters measure the complete polarization properties of a sample in the context of the Stokes vector formalism. Many such instruments are designed for use with quasi-monochromatic illumination, for reasons of calibration simplicity and speed [1]. When spectrally resolved information is also needed, a common approach is to use the same instrumentation and simply step through the various wavelength bands [2]. This trades off temporal resolution for chromatic information and introduces the inconvenience of using scanning hardware (such as rotatable mounts).

We present a snapshot method for performing spectrally resolved Mueller matrix measurements of a sample, which avoids these difficulties. By use of frequency-domain interferometry, instead of a temporal resolution trade-off, we can trade with spectral resolution to achieve a complete measurement. By "snapshot" we do not mean to imply fast, since monochromatic systems are typically far faster. Rather, we mean that the complete measurements can be taken in a single integration period of a single detector array, with no moving or active parts in the system. The resulting instrument is potentially very compact.

The basic layout of the snapshot Mueller matrix spectropolarimeter is shown in Fig. 1. The device concept extends the method of channeled spectropolarimetry [3] to not only analyze polarized light, but also to generate it [4,5]. The sample is thus illuminated by a polarization state that varies spectrally, allowing a simultaneous measurement of the output polarization states of the sample for many input polarization states. If the Mueller matrix of the sample varies only slowly with wavelength, then the measurements will not overlap and can be accurately recovered.

Using the Mueller calculus to model the propagation of polarization states through the system, we first write $\mathbf{s}_{\text{in}}(\sigma)$ as the Stokes vector for the spectrum of light incident on the first polarizer ($\sigma \equiv 1/\lambda$ is the wavenumber). $\mathbf{R}_n(\theta_n, \delta_n)$ represents the Mueller matrix for the nth retarder element, with retardance δ_n and fast axis orientation angle θ_n. Likewise, $\mathbf{P}_n(\theta)$ is the matrix for the nth polarizer, with transmission axis at angle θ. $\mathbf{M}$ is the Mueller matrix of the sample itself. (Note that the quantities δ_n and m_{ij} are functions of wavenumber σ; to clarify the expressions, the explicit dependence will not be shown.) The light in front of the spectrometer is therefore given by

$$\mathbf{s}_{\text{out}}(\sigma) = \mathbf{P}_2(0^\circ)\mathbf{R}_4(45^\circ, \delta_4)\mathbf{R}_3(0^\circ, \delta_3)\mathbf{M} \times \mathbf{R}_2(0^\circ, \delta_2)\mathbf{R}_1(45^\circ, \delta_1)\mathbf{P}_1(0^\circ)\mathbf{s}_{\text{in}}(\sigma). \quad (1)$$

Performing the matrix multiplications of Eq. (1), we obtain an irradiance $I(\sigma) = s_{\text{out},0}(\sigma)$ at the spectrometer of

$$\begin{aligned} I(\sigma) = \frac{s_{\text{in},0}(\sigma)}{4}\big(&m_{00} + m_{01}\cos\delta_1 + m_{02}\cos\delta_1\sin\delta_2 \\ &+ m_{03}\cos\delta_2\sin\delta_1 + m_{10}\cos\delta_4 \\ &+ m_{11}\cos\delta_1\cos\delta_4 + m_{12}\sin\delta_1\sin\delta_2\cos\delta_4 \\ &+ m_{13}\sin\delta_1\cos\delta_2\cos\delta_4 + m_{20}\sin\delta_3\sin\delta_4 \\ &+ m_{21}\cos\delta_1\sin\delta_3\sin\delta_4 \\ &+ m_{22}\sin\delta_1\sin\delta_2\sin\delta_3\sin\delta_4 \\ &+ m_{23}\sin\delta_1\cos\delta_2\sin\delta_3\sin\delta_4 \\ &- m_{30}\cos\delta_3\sin\delta_4 - m_{31}\cos\delta_1\cos\delta_3\sin\delta_4 \\ &- m_{32}\sin\delta_1\sin\delta_2\cos\delta_3\sin\delta_4 \\ &- m_{33}\sin\delta_1\cos\delta_2\cos\delta_3\sin\delta_4\big). \end{aligned}$$

Using d_n for the thickness of retarder R_n and $B_n(\sigma)$ for its birefringence, we can write the retardance terms as $\delta_n(\sigma) = 2\pi d_n \sigma B_n(\sigma)$. To obtain the Mueller matrix elements from the measured spectrum $I(\sigma)$, we first take its Fourier transform. With the proper choice of retarder thicknesses, the various matrix el-

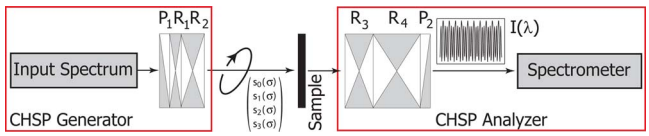

Fig. 1. (Color online) Basic layout of the snapshot Mueller matrix spectropolarimeter. Retarders 1 and 4 have their fast axes oriented at 45°, retarders 2 and 3 at 0°. Polarizers 1 and 2 both have their transmission axes oriented at 0°. CHSP, channeled spectropolarimeter.

ements are separated into independent channels in the Fourier domain. Inspired by the dual-rotating-retarder Mueller matrix polarimeter [6], we choose a 5:1 ratio of thicknesses for the pair of analyzing retarders to the generating pair to give a compact result. Further selecting a 2:1 ratio of thicknesses for the retarders within each pair gives a set of thicknesses that we designate as a 1-2-5-10 configuration, for the relative thicknesses of R_1 through R_4.

The optical path difference (OPD) in waves, for retarder R_n, is defined as $\mathrm{OPD}_n(\sigma)=(1/2\pi)\delta_n(\sigma)$; the mean OPD is then $\mathrm{OPD}_n(\sigma_0)$ for σ_0, the mean wavenumber in the spectrum. The OPDs of the channels in the Fourier domain are illustrated in Fig. 2. The Mueller matrix elements encoded within each channel are listed in Table 1.

Extracting the Mueller matrix involves windowing a channel (or a set of channels) in the Fourier domain and performing an inverse transform to obtain the spectrally resolved elements. Table 2 lists the steps needed to recover all 16 matrix elements. Figure 3 shows a simulated measurement of a polymer achromatic quarter-wave retarder (based on measurements in our lab of one such retarder from Meadowlark Optics Inc.). This element provides an interesting object for spectropolarimetry because of the nonlinear spectral variation of both retardance δ and fast-axis orientation angle θ. The simulation uses a blackbody spectral source for the 400–700 nm range and calcite retarders with 1, 2, 5, and 10 times the thickness of 0.265 mm. The birefringence is derived from the standard Sellmeier coefficients for the ordinary and extraordinary rays in quartz crystal. The detector is assumed to have 2000 spectral resolution elements, digitized to 10 bit range and corrupted by Poisson noise.

A practical concern for implementing this instrument is whether it is sensitive to misalignment and manufacturing tolerances. To analyze these issues, we ran the previously described simulation for perturbed system parameters $\tilde{\theta}_n=\theta_n+\Delta\theta$ and $\tilde{\delta}_n=\delta_n+\Delta\delta$, with azimuth error $\Delta\theta$ and retarder thickness error $\Delta\delta$. The calibration procedure for a channeled spectropolarimeter generally involves assuming the azimuth angles to be without error and using a reference spectrum measurement to calibrate the retardances $\delta_n(\sigma)$. In a Mueller matrix spectropolarimeter, a no-sample measurement likewise allows

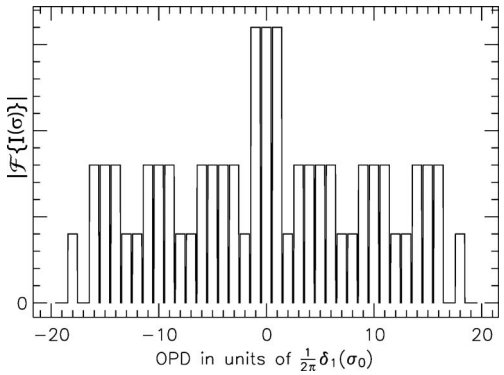

Fig. 2. Fourier domain, 37 channels C_n.

Table 1. Fourier-Domain Channels C_n Encoding the Mueller Matrix Elements for the 1-2-5-10 Configuration[a]

OPD (C_n)	Channel Content $\times(64/s_{\mathrm{in},0})$
0	$16m_{00}$
±1	$8m_{01}+4m_{02}\pm4im_{03}$
±2	$-m_{22}\pm im_{23}\mp im_{32}-m_{33}$
±3	$-4m_{02}\mp4im_{03}$
±4	$2m_{21}+m_{22}\mp im_{23}\pm2im_{31}\pm im_{32}+m_{33}$
±5	$4m_{20}\pm4im_{30}$
±6	$2m_{21}+m_{22}\pm im_{23}\pm2im_{31}\pm im_{32}-m_{33}$
±7	$-2m_{12}\pm2im_{13}$
±8	$-m_{22}\mp im_{23}\mp im_{32}+m_{33}$
±9	$4m_{11}+2m_{12}\mp2im_{13}$
±10	$8m_{10}$
±11	$4m_{11}+2m_{12}\pm2im_{13}$
±12	$m_{22}\mp im_{23}\mp im_{32}-m_{33}$
±13	$-2m_{12}\mp2im_{13}$
±14	$-2m_{21}-m_{22}\pm im_{23}\pm2im_{31}\pm im_{32}+m_{33}$
±15	$-4m_{20}\pm4im_{30}$
±16	$-2m_{21}-m_{22}\mp im_{23}\pm2im_{31}\pm im_{32}-m_{33}$
±18	$m_{22}\pm im_{23}\mp im_{32}+m_{33}$

[a]The OPD numbers listed for the channels are given in terms of multiples of $\mathrm{OPD}_1(\sigma_0)$, the mean OPD of the thinnest retarder.

calibration of the $\delta_n(\sigma)$. For azimuth errors, the approach needs to be more complex, but the effect of ignoring them is simply that azimuth errors in system elements cannot be differentiated from changes in the sample. Thus, for example, an azimuth error of 0.3° of a polarizer can appear as a 0.3° azimuth change in the sample.

The primary restriction on the kind of measurement that can be made accurately with this approach is that the spectral variation of all Mueller matrix elements must vary slowly enough that none of the channels overlap in the Fourier domain. The width of each channel is the mean OPD of the thinnest retarder. The effective Nyquist limit of the Mueller matrix elements is thus given not by the sampling rate of the spectrometer but by the sampling rate of a single channel. If the retarder thicknesses are chosen such that the Nyquist limit of the spectrometer coin-

Table 2. Spectrally Resolved Mueller Matrix Elements $m_{ij}(\sigma)$ Obtained by Operating on Spectral-Domain Channels c_n[a]

$m_{00}(\sigma)=4c_0$	$m_{20}(\sigma)=16\,\mathrm{Re}\{c_5\}$
$m_{01}(\sigma)=8(c_1+c_3)$	$m_{21}(\sigma)=32\,\mathrm{Re}\{c_2+c_4\}$
$m_{02}(\sigma)=-16\,\mathrm{Re}\{c_3\}$	$m_{22}(\sigma)=-32\,\mathrm{Re}\{c_2+c_8\}$
$m_{03}(\sigma)=16\,\mathrm{Re}\{c_1\}$	$m_{23}(\sigma)=32\,\mathrm{Im}\{c_2-c_8\}$
$m_{10}(\sigma)=8c_{10}$	$m_{30}(\sigma)=16\,\mathrm{Re}\{c_5\}$
$m_{11}(\sigma)=16(c_7+c_9)$	$m_{31}(\sigma)=16\,\mathrm{Im}\{c_2+c_4+c_6+c_8\}$
$m_{12}(\sigma)=-32\,\mathrm{Re}\{c_7\}$	$m_{32}(\sigma)=-32\,\mathrm{Im}\{c_2+c_8\}$
$m_{13}(\sigma)=32\,\mathrm{Im}\{c_7\}$	$m_{33}(\sigma)=32\,\mathrm{Re}\{c_8-c_2\}$

[a]These are given in terms of the Fourier-domain channels by $c_n(\sigma)=[1/s_{\mathrm{in},0}(\sigma)]\mathcal{F}^{-1}\{w(\mathrm{OPD})C_n(\mathrm{OPD})\}$, for windowing function w.

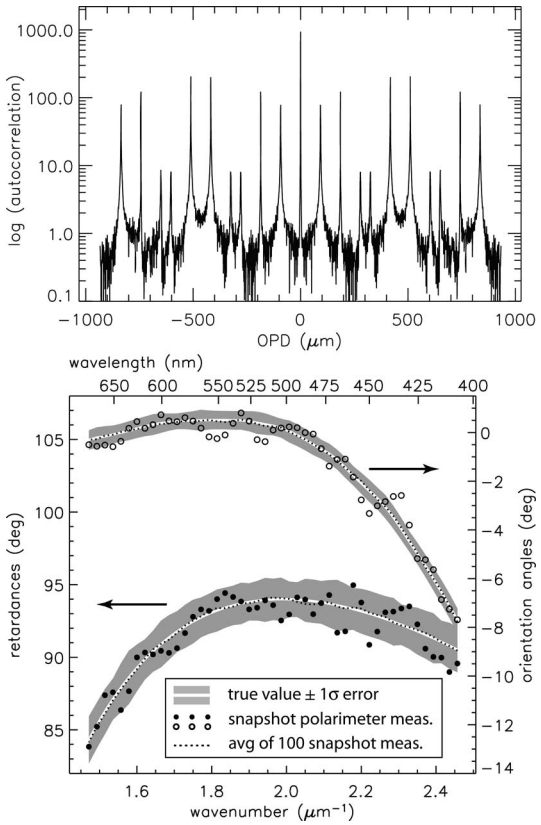

Fig. 3. Simulated measurement of an achromatic polymer retarder using a snapshot Mueller matrix polarimeter. Upper figure: the Fourier-domain representation of the measured spectrum. Lower figure: the retardance $\delta(\sigma)$ and orientation angle $\theta(\sigma)$ of the sample reconstructed from the measured Mueller matrix elements. The error bars are obtained from the standard deviation of data taken over 100 instances of Poisson noise.

cides with the edge of the highest-frequency channel, the analysis implies a loss in spectral resolution by a factor of 37 (for 18 positive and 18 negative channels plus the DC channel). This can place stringent requirements on readily available spectrometers to produce a useful spectral resolution for the Mueller matrix. For example, the highest-resolution visible-light spectrometer available through Ocean Optics Inc. has 2000 resolution elements, with which Mueller matrix elements can thus be measured with $2000/37 \sim 54$ spectral resolution elements.

Because of its snapshot capability, this technique could be employed in some applications where moving parts are difficult to use and the trade-off in spectral resolution is acceptable, though it is limited to measuring samples whose Mueller matrix elements vary only slowly with wavelength (i.e., each Mueller matrix element's spectral dependence must be band-limited to within the width of a single channel). Examples include *in situ* ellipsometry of thin films, *in vitro* biomedical imaging, or underwater measurement of samples.

Polarimetry is a relatively small field, in part because the instrumentation required for polarization measurements is too complicated for casual use. A compact snapshot instrument may allow access to users whose budgetary and time constraints have prevented them from making use of polarization in their research.

This work was supported in part by Department of Defense contract DAAE07-02-C-L011.

References

1. D. H. Goldstein, Appl. Opt. **31**, 6676 (1992).
2. L. Jin, K. Takizawa, Y. Otani, and N. Umeda, Opt. Rev. **12**, 281 (2005).
3. K. Oka and T. Kato, Opt. Lett. **24**, 1475 (1999).
4. T. Wakayama, Y. Otani, and N. Umeda, Proc. SPIE **5888** (2005).
5. H. Okabe, M. Hayakawa, H. Naito, A. Taniguchi, and K. Oka, Opt. Express **15**, 3093 (2007).
6. R. M. A. Azzam, Opt. Lett. **2**, 148 (1978).

Snapshot Mueller matrix spectropolarimeter: erratum

Nathan Hagen,[1] Kazuhiko Oka,[2] and Eustace L. Dereniak[1]

[1]*College of Optical Sciences, University of Arizona, 1630 E. University Boulevard, Tucson, Arizona 85721, USA*

[2]*Division of Applied Physics, Graduate School of Engineering, Hokkaido University, Sapporo 060-8628, Japan*

**Corresponding author: nhagen@optics.arizona.edu*

Received April 17, 2013;
posted April 17, 2013 (Doc. ID 187686); published May 10, 2013

We correct an error in one of the equations in our original manuscript.

OCIS codes: (120.2130) Ellipsometry and polarimetry; (120.5410) Polarimetry; (260.5430) Polarization; (300.6190) Spectrometers.

http://dx.doi.org/10.1364/OL.38.001675

The second equation in our original manuscript [1] contains a typo in which $m_{02} \sin \delta_1 \sin \delta_2$ appears as $m_{02} \cos \delta_1 \sin \delta_2$. Thus, the correct form of the equation should be

$$\begin{aligned} I(\sigma) = \frac{s_{\text{in},0}(\sigma)}{4} (& m_{00} + m_{01} \cos \delta_1 + m_{02} \sin \delta_1 \sin \delta_2 \\ & + m_{03} \cos \delta_2 \sin \delta_1 + m_{10} \cos \delta_4 \\ & + m_{11} \cos \delta_1 \cos \delta_4 + m_{12} \sin \delta_1 \sin \delta_2 \cos \delta_4 \\ & + m_{13} \sin \delta_1 \cos \delta_2 \cos \delta_4 + m_{20} \sin \delta_3 \sin \delta_4 \\ & + m_{21} \cos \delta_1 \sin \delta_3 \sin \delta_4 \\ & + m_{22} \sin \delta_1 \sin \delta_2 \sin \delta_3 \sin \delta_4 \\ & + m_{23} \sin \delta_1 \cos \delta_2 \sin \delta_3 \sin \delta_4 \\ & - m_{30} \cos \delta_3 \sin \delta_4 - m_{31} \cos \delta_1 \cos \delta_3 \sin \delta_4 \\ & - m_{32} \sin \delta_1 \sin \delta_2 \cos \delta_3 \sin \delta_4 \\ & - m_{33} \sin \delta_1 \cos \delta_2 \cos \delta_3 \sin \delta_4). \end{aligned}$$

The remainder of the manuscript is unaffected by the change.

Our thanks to Andrey Alenin for pointing out the error.

Reference

1. N. Hagen, K. Oka, and E. L. Dereniak, Opt. Lett. **32**, 2100 (2007).

